

Effects of processing conditions on flash sintering of commercial ZrN

Amirali Eskandariyun | Suprabha Das  | Diego Dubois | Kiyana Saeedian | Andriy Durygin | Vadym Drozd | Zhe Cheng

Mechanical and Materials Engineering Department, Florida International University, Miami, Florida, USA

Correspondence

Zhe Cheng, Mechanical and Materials Engineering Department, Florida International University, Miami, FL, USA.
 Email: zhcheng@fiu.edu

Funding information

U.S. Department of Energy (DOE), Office of Science, Basic Energy Science, Grant/Award Number: DE-SC0022152; Presidential Fellowship award by Florida International University Graduate School

Abstract

Flash sintering (FS) is a potentially rapid and low-cost manufacturing technique for advanced ceramics. There are still many unknowns about ceramic FS, especially for highly conductive high-temperature ceramics (HTC), which often display decreased bulk conductivity with increasing temperature. This study qualitatively characterizes the flash behavior of highly conductive HTC materials using zirconium nitride (ZrN) as an example. The effects of processing parameters (e.g., DC voltage/electrical field strength, voltage ramp rate, post-flash holding time, mechanical pressure, sample milling, and choice of electrode materials) on ZrN flash behavior are also qualitatively studied and linked to samples microstructure and hardness. It is observed that best densification was achieved using 5 min Spex-milled ZrN powder under 25 MPa of applied pressure and constant 8 V DC. The potential mechanism for ZrN FS and the similarity and difference from FS of conventional oxides like YSZ have been proposed based on experimental observations, and the directions for future research are also pointed out.

KEY WORDS

flash sintering, high-temperature ceramics, pressure, zirconium nitride

1 | INTRODUCTION

Zirconium nitride (ZrN) is a high-temperature ceramic (HTC) with a high melting point of $\sim 3000^\circ\text{C}$ ¹ and good hardness and corrosion/wear resistance.² Due to these exceptional properties, ZrN is used as coatings for machining tools, and it is also a candidate material for extreme environments, such as refractories and aerospace applications.^{1,2} Unlike many other ceramics, ZrN shows metallike electrical and thermal conductivity,³ which broadens its applications. However, due to the strong covalent bonds and low self-diffusion coefficient of ZrN, and HTCs in general, it can be challenging to densify their powders using conventional sintering methods⁴: It usually

requires high temperatures and significant dwell time,⁴ which is not very economically and energy efficient. Therefore, researchers are constantly pursuing novel methods to shorten the time and reduce the energy required to consolidate ZrN as well as other HTCs. Among those techniques, field-assisted sintering techniques (FAST) in different embodiments have attracted the most interest.⁵

Flash sintering (FS) is one of the FAST techniques that enable very rapid and low-cost consolidation of ceramics.^{6,7} It was initially demonstrated about a decade ago by Raj et al.^{8,9} It has been successfully adopted for sintering many oxides such as Y_2O_3 -stabilized ZrO_2 (YSZ)¹⁰ within a few minutes or even seconds. As shown in Figure 1A,⁹ those studies mostly adopt a pressureless

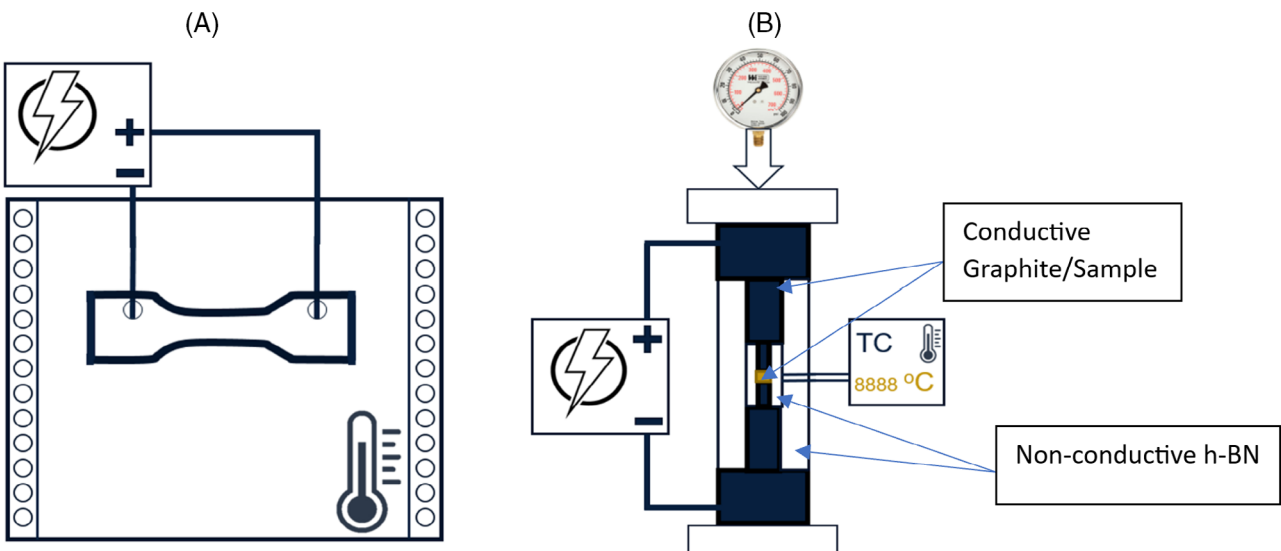


FIGURE 1 (A) Conventional pressure-less flash sintering (FS) using dog-bone-shaped samples, (B) pressure-assisted sinter-forging type FS (present study).

configuration with a dog-bone-shaped sample often placed inside a furnace at an elevated temperature in the range of 300–1300°C.¹¹ Although dense ceramics are obtained, it may require significant energy to preheat the furnace and trigger the flash event, especially for low conductivity oxides such as YSZ or MgO-doped Al₂O₃.

In recent years, FS in the sinter-forging configuration has also been demonstrated. This configuration, also called pressure-assisted flash sintering (PAFS), uses an electrical field as well as a low pressure (e.g., ~10–50 MPa) to densify ceramic powders, even without preheating or pre-compacting,^{12–15} as shown in the schematic in Figure 1B.¹⁵ Such PAFS has been adopted in several institutions and demonstrated for both oxides¹⁵ and non-oxides, such as transition metal carbides, borides, and nitrides.^{14,16–22} Compared with classical FS with DC electrical field strength in the range of ~10–1000 V/cm and current density in the range of ~0.1–50 mA/mm,^{2,23} sinter-forging type FS has been applied to highly conductive ceramics such as hafnium–zirconium diboride¹⁸ and tungsten carbide,^{19–21} with low electrical field strength in the range of ~1–30 V/cm and very high current density in the range of ~10–50 A/mm² (or 10,000–50,000 mA/mm²).

No matter which configuration, FS experiment typically consists of three stages. The first is called (pre-flash) *incubation* with extremely low current and power dissipation. The second stage is the *flash* event in which current increases by tens or hundreds of times with small or no change in the applied voltage (or electrical field strength). The sudden drop in sample electrical resistance leads to a drastic increase in power dissipation ($P = U^2/R$ under constant voltage) and potentially other effects. Accordingly, the sample heats up extremely fast and experiences

rapid densification. The third or the last stage is called *steady-state* or post-flash holding. It occurs after the power supply transitions from voltage control (constant or slow, linear ramp) to current control (normally constant current mode). The duration of the flash event, which is responsible for most of the densification process, ranges from a few seconds to tens of seconds, depending on electrical field strength and the sample.

Most studies in the literature on FS have been carried out on oxides such as YSZ¹⁰ and they suggest several possible reasons for the flash event. For example, it is well known that many oxides such as YSZ and ZnO show higher electrical conductivity with increasing temperature, following Arrhenius-type relationship,²⁵ as shown in Figure 2. For such oxides, even without considering other factors, the application of a constant voltage (or electrical field strength) would induce electrical current (density) and Joule heating (preheating might be needed to generate measurable current), which increases sample temperature. The increased temperature, in turn, leads to a higher material electrical conductivity. Under constant voltage conditions, higher electrical conductivity (or lower resistivity) means higher current (density) will pass through the sample, leading to more Joule heating and even higher temperatures. This *snowball* effect eventually leads to thermal runaway and the flash event,²⁶ which must be limited by transitioning the power supply from voltage control into current control to prevent damage to the sample (and equipment). There are some additional explanations for the flash event. For example, some proposed that grain boundaries or the contact regions between particles are more resistive and thus the concentration of Joule heating at those places will result in much higher temperatures

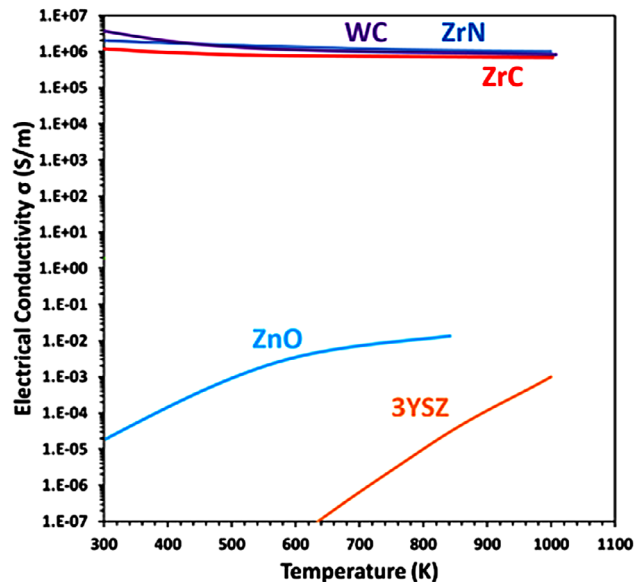


FIGURE 2 Plot of *bulk* electrical conductivity (in log scale) versus temperature for oxides of 3% mol Y_2O_3 -doped ZrO_2 (3YSZ) and ZnO as well as highly conductive high-temperature ceramics (HTC) such as ZrN , ZrC , and WC .^{20,35–38}

than bulk values^{27,28}; some hypothesized that the flash event occurs due to the avalanche of the Frenkel (e.g., oxygen vacancy—oxygen interstitial) pairs.^{29,30} Other factors include (partial) electrochemical reductions^{31,32} and dielectric breakdown.^{33,34}

Although a few studies have been carried out on FS of highly conductive HTCs, such as borides, carbides, and nitrides,^{14,16–21} there have not been many efforts to systematically characterize the detailed flash *behavior* for these materials and delve into possible *mechanisms*. As shown in Figure 2, the conductivity-temperature relationship of several highly conductive HTCs including ZrN is like metals, meaning when temperature increases, ZrN *bulk conductivity* would decrease,³ which is opposite to that for YSZ and would, in theory, *work against* the FS phenomenon. However, as mentioned, FS has indeed been demonstrated for highly conductive HTC including Tungsten Carbide (WC),^{19–21} $(\text{Hf}_{0.5}\text{Zr}_{0.5})\text{B}_2$,¹⁸ as well as ZrN .¹⁶

Such an apparent contradiction motivates the current FS study of HTC using ZrN as an example. It aims to make up for the knowledge gap in the literature by characterizing the behavior of the flash event for ZrN and, *qualitatively*, answer some basic questions. For example, how do voltage influence the flash event? Linearly or nonlinearly? What is the effect of powder milling? Is there repeated flash for the same sample? The observations are linked with possible physical/chemical processes for such materials and the similarities and differences from oxides FS are also discussed. It noted that additional investigation focusing on the *kinetic aspect* of ZrN FS including more precise quan-

titative analysis of samples' detailed microstructure and microchemical characteristics is still ongoing and will be reported in a later study.

2 | EXPERIMENTAL PROCEDURES

2.1 | Flash sintering setup

The homemade PAFS setup at Florida International University has been described before.¹⁷ Essentially, it consists of a DC power supply (HP Agilent 6671A, 8 V, 220 A) and a pneumatic cylinder (McMaster-Carr double-acting round body air cylinder) to apply mechanical pressure (varying from ~ 3 to 30 MPa on the sample). Figure 3A is a photo of the actual setup, whereas parts (b) and (c) of Figure 3 are schematics of the sample assembly. The pre-compacted short cylindrical green sample (e.g., 0.1 g ZrN powder, 3.1 mm diameter, and ~ 2.5 mm thickness from dry pressing) was enclosed within insulating h-BN tubes and contacted by the top and bottom graphite electrodes. The sample assembly force electrical current to only go through the sample, distinguishing it from typical spark plasma sintering (SPS),³⁹ where the exact current pathway is determined by the electrical resistance of both the tool (i.e., graphite die set) and the sample. (If the powder compact in SPS exhibits high resistance, current will travel almost exclusively through the graphite die body. On the other hand, upon heating up and sample densification, if the sample resistance drops significantly, part of the current may start to pass through the sample, while the rest continues to pass through the graphite die.)

The FS setup has computer control. It does have several major limitations: First, it could not accurately measure sample temperature due to issues such as tip melting for thermocouples and blockage of the center hot zone for the pyrometer (infrared) method. Second, the precise shrinkage versus time or temperature data also could not be measured. This was due to factors such as (i) the very small sample size (often ~ 0.1 g or less in weight) and (ii) the lack of a mechanism for inserting a reference (or standard) material at the same temperature to correct for effects such as thermal expansion.

Nevertheless, when enough DC voltage (e.g., 8 V or ~ 32 V/cm) was applied, the flash or the rapid increase in current appear *instantaneously* (i.e., almost at zero time) *without* preheating in this study, indicating the flash of ZrN happens at around room temperature before significant heating could occur. In addition, due to the fact the sample was enclosed in h-BN sleeves with graphite top and bottom electrodes, non-oxide ceramics (e.g., carbides, borides, and nitrides) had been flash sintered in air with negligible oxidation. The 3 mm inner electrodes, graphite or Mo metal,

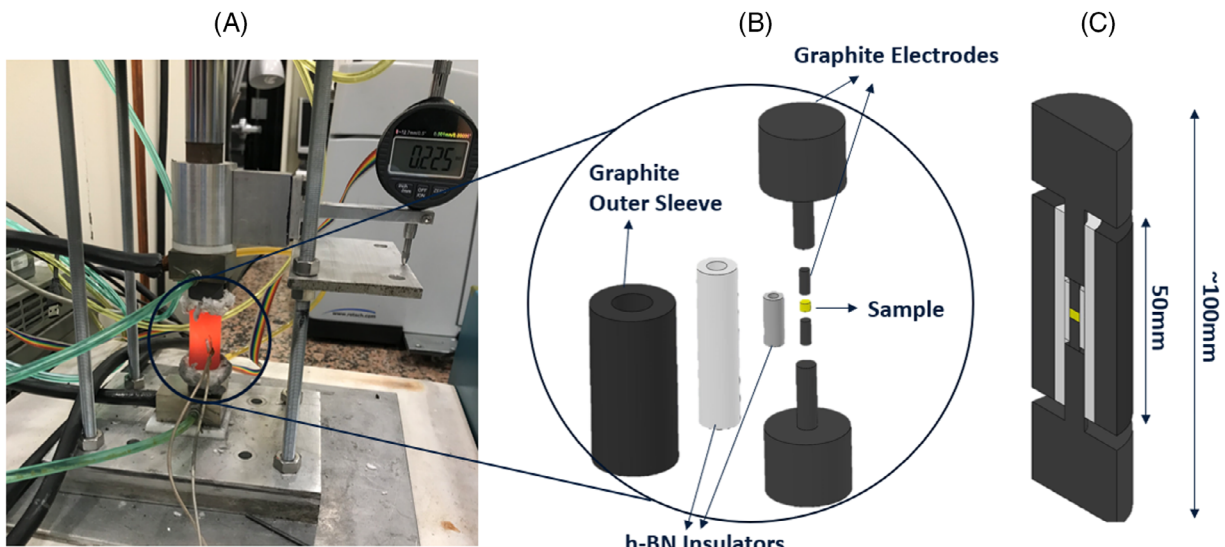


FIGURE 3 (A) Photo of the homemade flash sintering setup. (B) A schematic showing parts in the sample assembly for flash sintering (FS), including one graphite outer sleeve (25 mm O.D., 12.5 mm I.D.), one outer h-BN tube (12.5 mm O.D., 6.3 mm I.D.), two outer graphite electrodes (6.3 mm O.D. at the small end; 25 mm O.D. at the large end), one inner h-BN tube (6.3 mm O.D., 3.1 mm I.D.), two inner graphite electrodes (3.1 mm O.D.), as well as the sample (3.1 mm O.D.). (C) Schematic exposing an axial cross section of the sample assembly for FS. Note electrical current is forced to only pass through the sample as it is enclosed inside the electrically insulating h-BN tube(s).

also survived the process, whereas oxidation was indeed observed for the outer graphite sleeve. That the sample was enclosed also helped reduce heat loss, which is beneficial in the sintering process.

2.2 | As-received commercial ZrN powder and mechanical milling

For this research we used commercial ZrN powder (Alfa Aesar 12138, 99.5% metal basis excluding Hf, Hf < 3%), which contains ~6.0 wt.% of tetragonal-phase ZrO_2 impurity based on Rietveld refinement (see Figure 4). As discussed later, despite the presence of t- ZrO_2 impurity, presumably as oxide shells covering ZrN particles, FS of commercial ZrN powder using homemade setup has been demonstrated, yielding relative density of >~90% in a couple of minutes. Scanning electron microscopy (SEM) image for the as-received commercial ZrN powder (see Figure 5) shows agglomerated particles with a size of ~1–20 μm , which is quite large. (Further characterization using advanced tools such as X-ray Photoelectron Spectroscopy (XPS), oxygen analysis by LECO corporation instrument, as well as High-Resolution Transmission Electron Microscopy/ Energy Dispersive X-ray Spectroscopy (HR-TEM/EDS) to precisely determine the oxygen content and surface chemistry of the ZrN powder will be carried out in future.) For some FS experiments, mechanical milling of the commercial ZrN power using SPEX Sample prep (8000D-115 Mixer/Mill) was carried out. Typically, 1 g

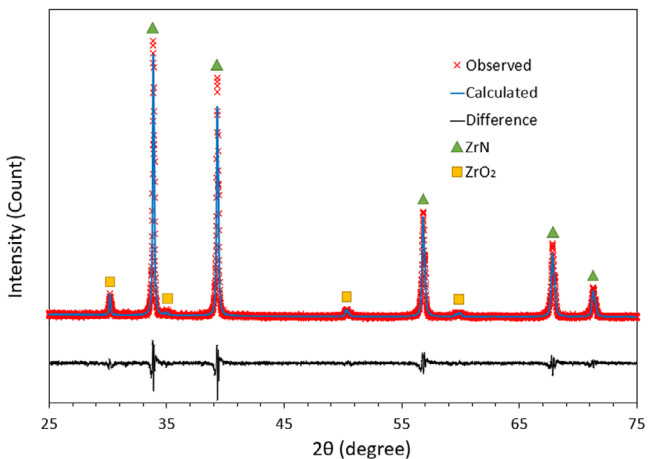


FIGURE 4 Rietveld refinement for the as-received commercial ZrN powder showing ZrO_2 impurity of ~6 wt.%.

of ZrN powder is loaded into the stainless-steel jar with a stainless-steel ball were used to mill the powder for 5 min in air before the FS experiment.

2.3 | Flash sintering experiments

In order to qualitatively reveal the effect of different processing parameters on the occurrence of the flash event and ZrN densification, a series of experiments have been carried out, and the processing parameters investigated include:

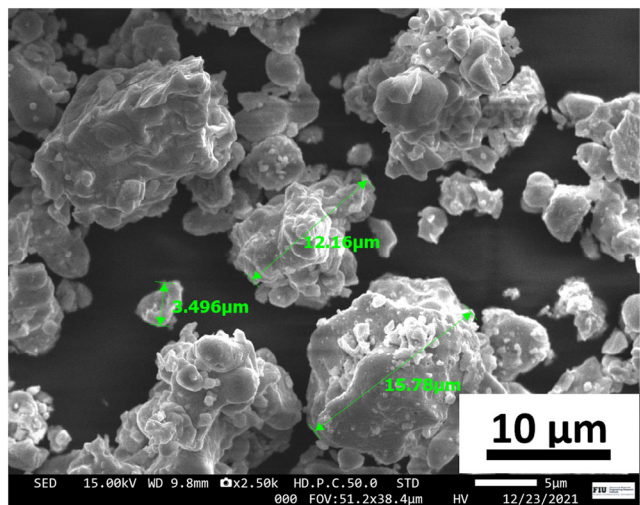


FIGURE 5 Scanning electron microscopy (SEM) of the as-received commercial ZrN powder.

- 1) Applied voltage (electrical field strength) and voltage ramp rate
- 2) Post flash holding time
- 3) Applied mechanical pressure
- 4) Powder milling
- 5) Electrode material
- 6) Repeated flash

For each set of experiments, only one parameter was varied, and all others were kept constant as much as possible. Typically, the amount of powder used was 100 mg. Other than studying the effect of pressure, the samples had been pre-compacted under \sim 2000 MPa in a 3.1 mm die for 30 s. (It is noted that the 2000 MPa pressure was generated by applying a pressure of 6.2 MPa or 900 psi using a 65 mm diameter cylinder on the 3.1 mm diameter sample. Such pressure for cold pressing was higher than ideal and might have caused some damage to the die set.) During FS, the applied external pressure on the sample was typically fixed at 15 MPa to maintain electrical contacts. (Lower pressure was also used to investigate the pressure effect.) The FS process was monitored by a computer program measuring real-time electrics (voltage/field strength and current). After FS, the densified samples were extracted (by breaking the sample assembly) for characterization.

2.4 | Sample characterization

The composition for the flash sintered ZrN sample has been verified using both XRD and EDS in an earlier publication.¹⁶ SEM was carried out using JSM-F100 (JEOL) for both commercial ZrN powder (see Figure 5) and flash-sintered samples for microstructure analysis. Due to factors such as the very small sample size, the often-low

relative density, and resulting poor mechanical strength, porosity and grain size for flash sintered samples were not obtained using conventional methods (e.g., Archimedes method). Instead, both porosity and average grain size were estimated from the SEM of samples' fractured surfaces. (It is noted that such estimates are rough and only serve as a first approximation. See supplemental for more details.) Vickers micro-indentation hardness test was carried out on some samples using LM810AT (LECO) at a loading of 2000 gf.

3 | RESULTS AND DISCUSSION

3.1 | Effects of applied voltage

3.1.1 | Constant voltage mode

For ZrN FS, the power supply can begin by operating in either the constant voltage mode or the linear ramping voltage mode. For constant voltage mode, Figure 6A shows the change of current versus time at different voltages for FS experiments carried out for the same amount of sample (0.1 g) at the same applied pressure (15 MPa). Voltage below \sim 5 V or initial electrical field of \sim 20 V/cm (initial sample thickness of \sim 2.5 mm; initial value used since the cylindrical samples experienced shrinkage in thickness during FS) would not trigger or initiate the flash for the ZrN samples inside the current setup: For example, when the applied voltage was 4 V, the current increased slightly from 3.65 A (0.48 A/mm^2) to 5.40 A (0.72 A/mm^2) but then plateaued and decreased afterward. When the voltage was 5 V, the current increased from 4.84 A (0.64 A/mm^2) to 22.84 A (3.0 A/mm^2) but again quickly plateaued and decreased afterward and even dropped suddenly to almost zero. As shown in Figure 6B, the maximum current versus applied voltage shows a clear nonlinear behavior: when voltage increased above 5 V, current increased dramatically; when the voltage doubled from 4 to 8 V, the post-flash steady-state current increased almost 30 times from \sim 5 A (0.66 A/mm^2) to \sim 143 A (19 A/mm^2). Such nonlinearity is characteristic of the FS behavior and is similar to that for oxide materials such as YSZ.

Another set of experiments were carried out to demonstrate the effects of electrical field by using samples with different mass, leading to varying thicknesses. In particular, samples of different masses including 0.04, 0.08, and 0.12 g were prepared by cold pressing. Then, the samples were flash sintered at the same voltage (8 V DC) and pressure (15 MPa), with post-flash holding of 400 s.

Figure 7 shows the change of current versus time for the three samples. From a first look, doubling or tripling of sample mass and, as a result, the green thickness would cause the electrical field to decrease accordingly under

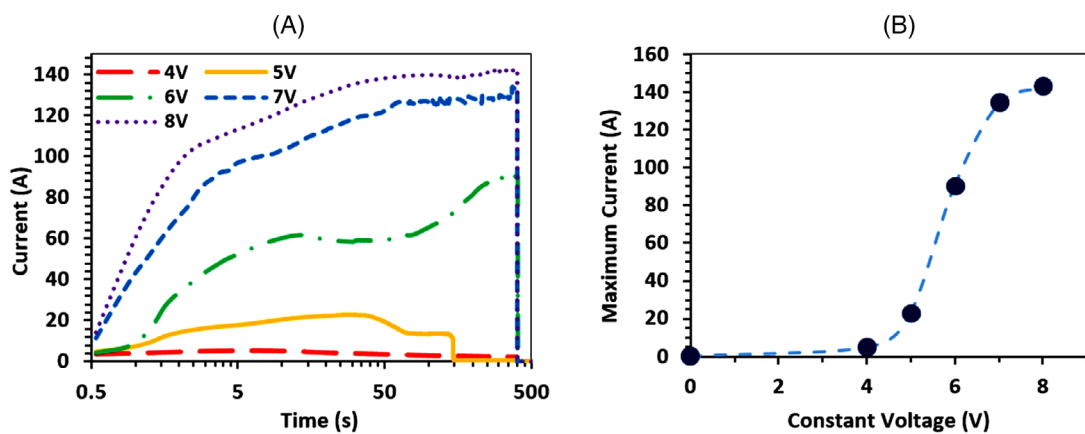


FIGURE 6 (A) Current versus time plot at different constant voltages and corresponding (B) maximum current versus respective constant voltage plot for ZrN flash sintering experiments showing the nonlinear flash behavior. Note the time for (A) is in log scale.

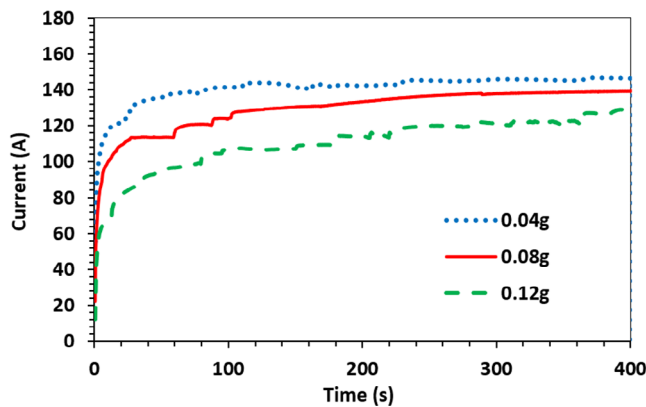


FIGURE 7 Current versus time for flash sintering (with 8 V DC and 15 MPa pressure) of 0.04, 0.08, and 0.12 g of commercial ZrN powder, respectively. All three samples have been pre-compacted before flash sintering at 8 V DC.

the same total voltage. However, the drop in max current was much less dramatic than expected from the drop in nominal initial electrical field: from ~ 146 A (19 A/mm 2) for 0.04 g (~ 1 mm) to 139 A (18 A/mm 2) for 0.08 g (~ 2 mm) to 129 A (17 A/mm 2) for 0.12 g (~ 3 mm). The total system resistance after reaching the steady state would be 8 V/ 146 A = 0.0548 Ω for 0.04 g, 8 V/ 139 A = 0.0576 Ω for 0.08 g, and 8 V/ 129 A = 0.0620 Ω for 0.12 g.

Assuming constant resistance for all other components (e.g., graphite electrodes and copper wiring) and contacts, a simple linear fitting gives an estimated sample apparent resistance of only ~ 0.0036 Ω for a 3.1 mm diameter, initially ~ 1 mm thick green ZrN sample (~ 0.04 g). Such an estimate means the FS process was complex in the current sinter-forging type set-up and there was significant resistance and voltage loss in either the (graphite) electrodes or at the contacts, for example, between graphite electrodes and the sample or between the graphite electrodes and the metal terminals. The corresponding apparent conductivity

is ~ 400 S/cm at elevated temperature (~ 1700 °C) for flash-sintered ZrN—still about one order of magnitude lower than bulk ZrN, possibly due to residual porosity as well as oxide impurity. Further study with inserted voltage probes will be applied to verify this above analysis and determine the resistance and voltage distribution in the system, as adopted by Mazo et al.^{19,20}

In terms of microstructure, consistent with the current-time result, the density for the 0.04 g sample appears higher with larger grains than for 0.08 and 0.12 g samples, as seen in the SEM of the three flash-sintered samples (Figure 8; estimated samples' relative density and grain size are given in Table S1; note those values are for information purpose only due to the limitations with sample quality and the analysis methods used).

3.1.2 | Linear ramping voltage mode

Another way to characterize the ZrN FS behavior is through linear ramping voltage. Figure 9 shows the change of applied voltage and current versus time for two ramp rates of 0.05 and 0.1 V/s, both from 0 to 8.1 V (the power supply's maximum). In both cases, as voltage linearly increases, current increases from zero first slowly, corresponding to the incubation stage. Then current increases at a faster rate, corresponding to the flash event or the sudden drop in sample resistance. For both samples, the critical voltage for the initiation of the flash event or the transition from constant resistance to rapidly dropping resistance is about the same at ~ 4.2 V. This agrees with the constant voltage experiments in which the flash occurs between 4 and 5 V. It should be mentioned that, consistent with the observation on WC,¹⁹ the mere occurrence of flash does not mean that the sample densification process is complete: high current and high power dissipation (at higher voltage, 8 V in this case) are required for densification.

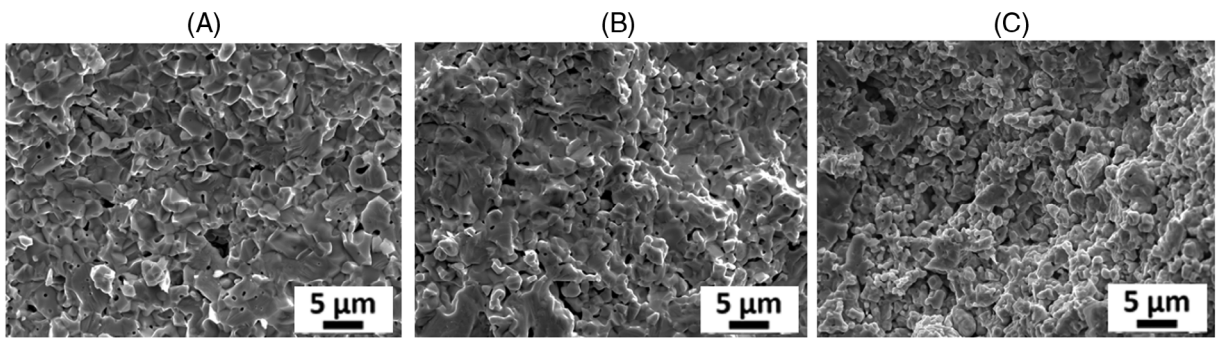


FIGURE 8 Scanning electron microscopy (SEM) micrographs of the fractured surfaces of the flash-sintered ZrN samples with different initial thicknesses (or powder mass): (A) 0.04 g, (B) 0.08 g, and (C) 0.12 g. The same 8 V DC voltage was applied, whereas the maximum current during flash sintering was 146 A (19 A/mm²), 139 A (18 A/mm²), and 129 A (17 A/mm²), respectively. (Estimated porosity and grain size are given in Table S1 for information purpose.)

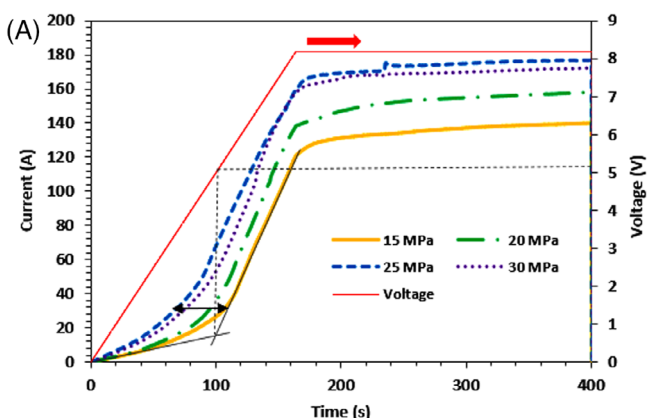
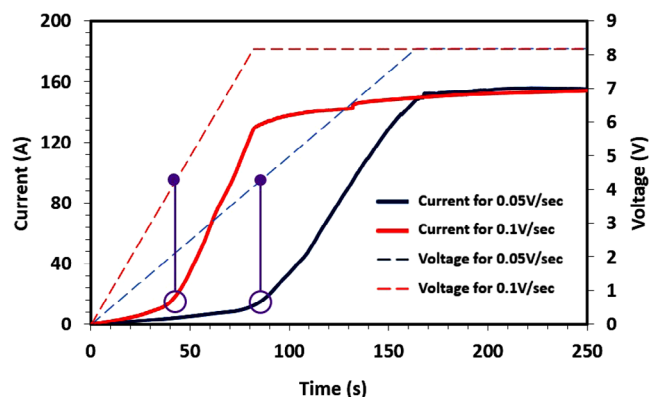


FIGURE 9 Current and voltage versus time for ramping voltage experiments. Note the onset of the flash event has been marked with solid circles to show the similar trigger or initiating voltage.

3.2 | Effects of pressure

For PAFS, obviously, pressure is applied to keep the contacts between electrodes and the sample. However, it is not clear how much pressure helps flash initiation and densification, especially given the pressure applied through the pneumatic cylinder during FS is below ~50 MPa—much lower than the pressure for pre-compacting the green pellets, as used in some studies.^{16,17} To understand the effect of pressure, a series of experiments were carried out using both loose ZrN powder (i.e., without pre-compacting) and pre-compacted samples. The possibility of ZrN FS without pressure was also explored by gradually reducing the applied pressure to a nearly negligible value. The following section presents the preliminary results.

Figure 10 shows the change of current versus time for ZrN FS carried out at different pressures from 15 to 30 MPa under a linear voltage ramp from 0 to 8 V DC

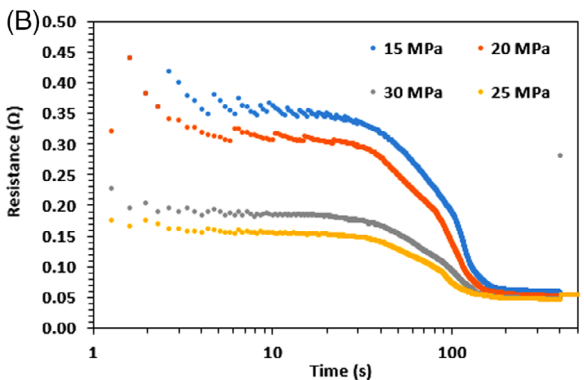


FIGURE 10 (A) Applied voltage and resulting current versus time for ZrN samples subject to different pressures during the flash sintering experiment. Note the samples were not pre-compacted for this set of experiments and the voltage was ramped linearly from 0 V at 0.05 V/s. The critical voltage was evaluated using the method shown with the gray lines. (B) Corresponding total resistance (i.e., applied voltage divided by current) over time at different applied pressures for the flash sintering experiments.

at 0.05 V/s without pre-compaction of the powder, meaning loose ZrN powder was directly loaded into the h-BN tube before the experiment. Consistent with the observation by Sglavo et al.,²⁰ within the conditions studied,

higher pressure leads to shorter incubation time before the flash. Because of the same linear voltage ramp (0.05 V/s), higher pressure appeared to cause flash to occur at a lower critical voltage: For example, at 15 MPa, the critical voltage occurred at ~5.15 V. The critical voltage decreased to ~3.8 V at 25 MPa. However, consider the green sample thickness $th_{25} = 3.45$ mm at 25 MPa, thickness at 15 MPa would be $th_{15} = th_{25} + \Delta = (3.45 + 0.4) = 3.85$ mm (Figure S1 shows displacement of 1.06 mm at 25 MPa vs. 0.66 mm at 15 MPa). The critical electrical field strength would be $\sim 5.15\text{ V}/th_{15} = 5.15\text{ V}/3.85\text{ mm} = 13.4\text{ V/cm}$ at 15 MPa versus $\sim 3.8\text{ V}/th_{25} = 3.8\text{ V}/3.45\text{ mm} = \sim 11.0\text{ V/cm}$ at 25 MPa. It shows that despite different pressures, the critical electrical field is not too different, indicating it is not the total voltage that determines the onset of the flash. Instead, it is more related to the critical field strength. On the other hand, Figure 10 does show the maximum current increases with increasing pressure up to ~25 MPa. This is explained as higher pressure leads to better densification, lower porosity, and higher apparent conductivity (not bulk conductivity since the samples contain different levels of porosity). As expected, when pressure increased further, its effect would seem to saturate: From ~25 to 30 MPa, no further benefits, that is, in terms of incubation time drop nor maximum current, are observed.

To explore the possibility of ZrN FS without applied mechanical pressure, pressure is decreased further from 15 to 3 MPa, with the same linear voltage ramp, and the results are presented in Figure 11. Flash did occur at pressure as low as 3 MPa with critical voltage of ~6.4 V (estimated sample thickness $th_3 = th_{25} + \Delta = (3.45 + 1.06) = 4.51$ mm; critical field strength ~14.2 V/cm). In fact, the transition from incubation to flash or transient is more abrupt with larger change in resistance. Extrapolating the data, the critical voltage at low pressure such as 0.1 MPa might be ~20 V, higher than the range available to the DC power supply used (i.e., 8 V) but finite. Considering the experiments start from loose powder without compaction, such results suggest that highly conductive HTC such as ZrN might go through conventional pressureless FS, in a way similar to FS for oxide materials such as YSZ. On the other hand, as in the range of 15–25 MPa, maximum current does increase with increasing pressure.

It should be noted that Mazo et al. investigated the effect of pressure on FS of WC.²⁰ They observed similar trend that higher pressure shortens the incubation. However, they did not observe the positive effect of higher pressure leading to higher max current, as observed in the current study. This is attributed to the difference in experimental setup: Mazo used pre-compacted pellet for pressure FS study, whereas the data in Figures 10 and 11 were obtained from loose powder without pre-compaction.

Figure 12 shows SEM micrographs of the fractured surfaces for samples flash sintered under different applied pressures without pre-compaction (see Figure 10). Consistent with expectation, below ~25 MPa, higher pressure led to higher max current and better densification.

3.3 | Effects of post-flash holding time

Consistent with our previous reports and the study by Sglavo,²⁰ FS for highly conductive HTC like ZrN can involve both FS and electrical resistance sintering, and the latter happens after the flash event when the power supply transitions from voltage control to constant current mode. Therefore, the effect of post-flash holding time from 35 to 400 s has been studied, all with constant 8 V DC and 15 MPa pressure, and the results are shown in Figure 13A (no powder Spex-milling, but all pre-compacted). It is noted that the $I-t$ curves show there was significant variability in (maximum) current, despite the same amount of sample and pressure and voltage. Such variations are attributed to variations in particle size (distribution) and resulting compaction in the green body. Another possible source of uncertainty is the quality of electrical contacts between different parts in the system including multiple graphite electrodes and metal (aluminum) terminals. The large variation indicates further optimization of the homemade FS setup is needed.

Nevertheless, Figure 13 shows that longer post-flash holding times generally led to better densification, with ZrN pellets sintered for 150 s or longer displaying decent hardness, whereas samples held for 35 and 50 s after the flash easily breaking up into powders. This is consistent with SEM for the fractured surfaces of these samples, as shown in Figure 13B–D: The sample held for 35 s after the flash showed high porosity, whereas the sample with post-flash holding of 200 s appeared much denser (estimated porosity and grain size are given in Table S1 for information purpose; same for below).

However, as the holding time increased to 400 s, further densification was not obvious: The 200 s sample appeared to have lower porosity and larger grains than the 400 s sample. Such an observation indicates the *maximum current (density)* (e.g., 167 A or 22 A/mm² for the 200 s sample in Figure 13C vs. 142 A or 19 A/mm² for the 400 s sample in Figure 13D) is likely more important than the post-flash holding time for FS densification of ZrN material.

Figure 14 shows SEM for some of the flashed sintered ZrN samples after polishing. They show improved grain connections and reduced porosity for samples with longer post-flash holding time. This is consistent with the measured Vickers hardness for the samples: As shown in Figure 15, the measured Vickers hardness increased from

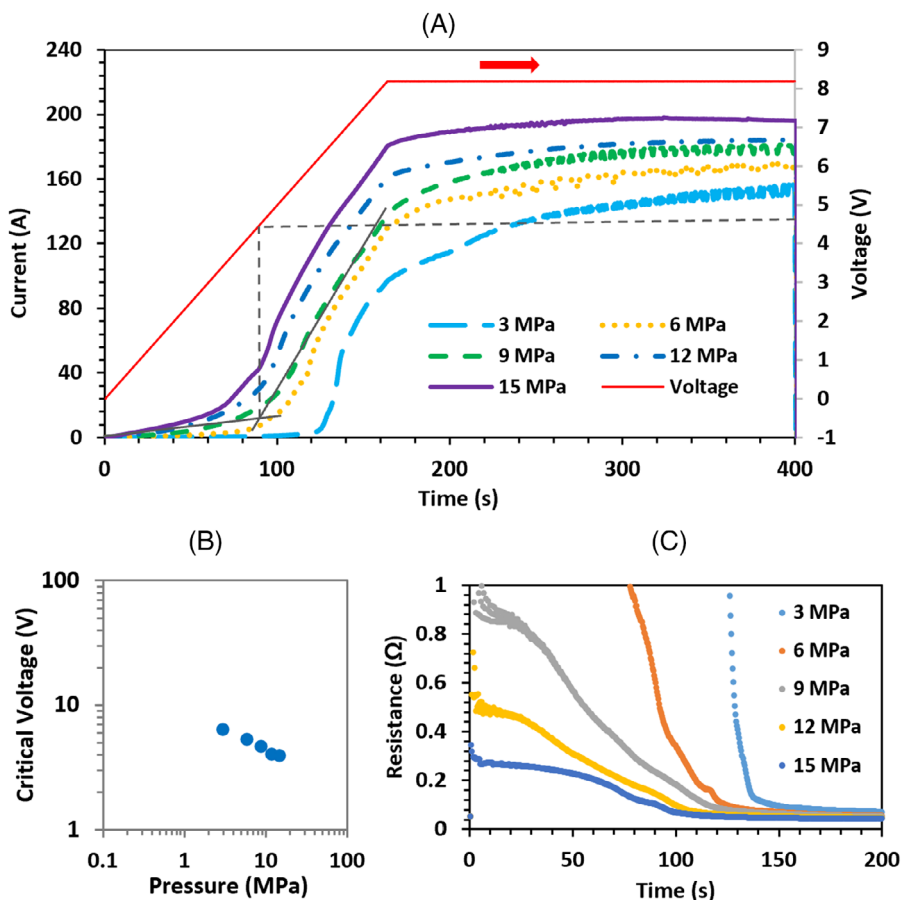


FIGURE 11 (A) Current and voltage versus time for flash sintering of samples without pre-compaction under applied pressures of 15 MPa and lower to evaluate the possibility of flash sintering without pressure. Voltage was ramped up linearly from 0 V to 0.05 V/s. Similar to Figure 10, the critical voltage was evaluated using the method shown with the gray lines. (B) Critical voltage (the voltage corresponding to the onset of the flash event) versus the applied pressure for flash sintering of ZrN powder. (C) Total resistance versus time for samples under different applied pressures.

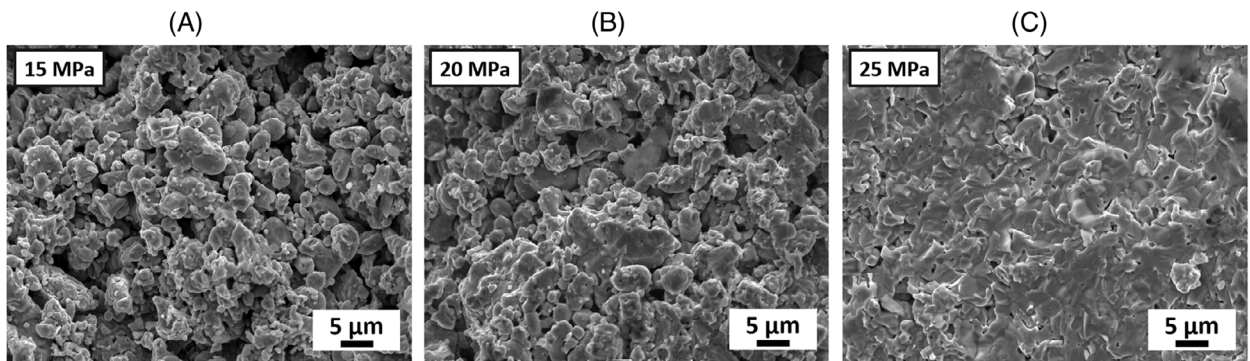


FIGURE 12 Scanning electron microscopy (SEM) micrographs of the fractured surfaces of the samples undergone different applied pressures of (A) 15 MPa (max 140 A, 18 A/mm²), (B) 20 MPa (max 158 A, 21 A/mm²), and (C) 25 MPa (max 176 A, 23 A/mm²), confirming the improvement in max current and resulting densification caused by the increase in pressure. Samples were prepared without powder Spex-milling and there was no pre-compaction, whereas the voltage was ramped up linearly. (Estimated porosity and grain size are given in Table S1 for information purpose.)

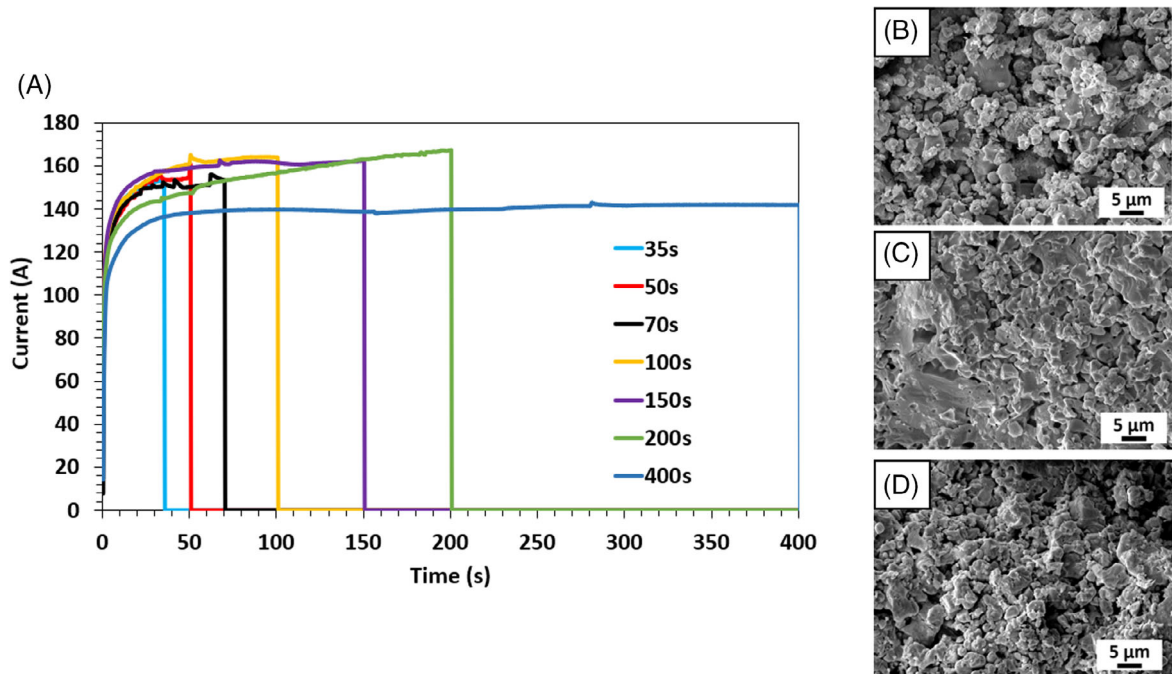


FIGURE 13 (A) Plot of current versus time for flash sintering of ZrN samples with different post-flash holding times, all under constant 8 V DC at 15 MPa pressure. (b-d) Scanning electron microscopy (SEM) micrographs for selected samples with different post-flash holding times and max current after flash sintering: (B) 35 s to 154 A (20 A/mm^2) max, (C) 200 s to 167 A (22 A/mm^2) max, and (D) 400 s to 142 A (19 A/mm^2) max. The samples were pre-compacted and prepared without Spex-milling. (Estimated porosity and grain size are given in Table S1 for information purpose.)

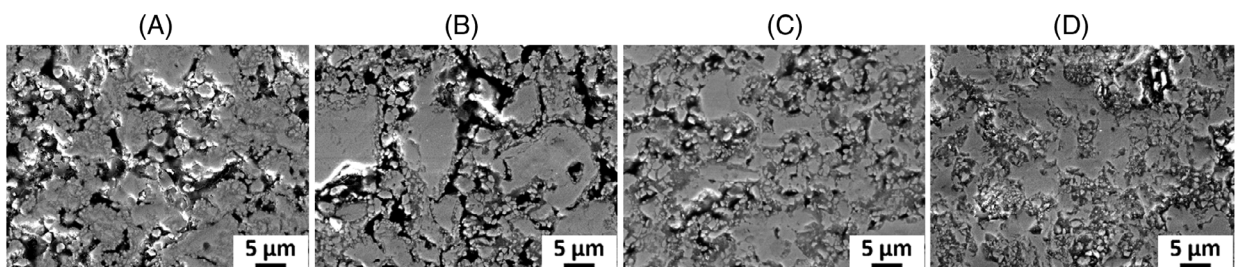


FIGURE 14 Scanning electron microscopy (SEM) micrographs of the polished surfaces for flash-sintered samples with different post-flash holding times of (A) 35 s, (B) 70 s, (C) 150 s, and (D) 200 s. All samples were flash sintered under constant 8 V DC and 15 MPa constant pressure. (Estimated porosity and grain size are given in Table S1 for information purpose.)

HV281 for the sample held for 35 s to HV948 for the sample held for 200 s. This confirms that although the flash event occurred on all the samples, the densification process continued after the flash. It is noted that although such post-flash dwell time required for densification is much shorter than conventional sintering and even SPS, but it may still be on the order of minutes. This is due to the limitation with the power supply used (e.g., only 8 V, 1600 W) as well as nonoptimal contacts (e.g., among the metal electrodes, the graphite electrodes, and the sample), and there might be significant room for future optimizations.

3.4 | Effect of powder mechanical milling

As mentioned earlier, the as-received commercial ZrN powder displayed flash behavior. However, it is observed that even with 8 V DC, high external pressures (up to 30 MPa), high current up to 167 A (or $\sim 22 \text{ A/mm}^2$), and post-flash holding time as long as 200 s, only limited densification has occurred (see Figures 8, 13, and 14). This is attributed to the very large particle size for the as-received commercial ZrN powder ($\sim 1\text{-}20 \mu\text{m}$), which limits the driving force for full densification. To overcome this, Spex-milling of the commercial ZrN powder was carried out to

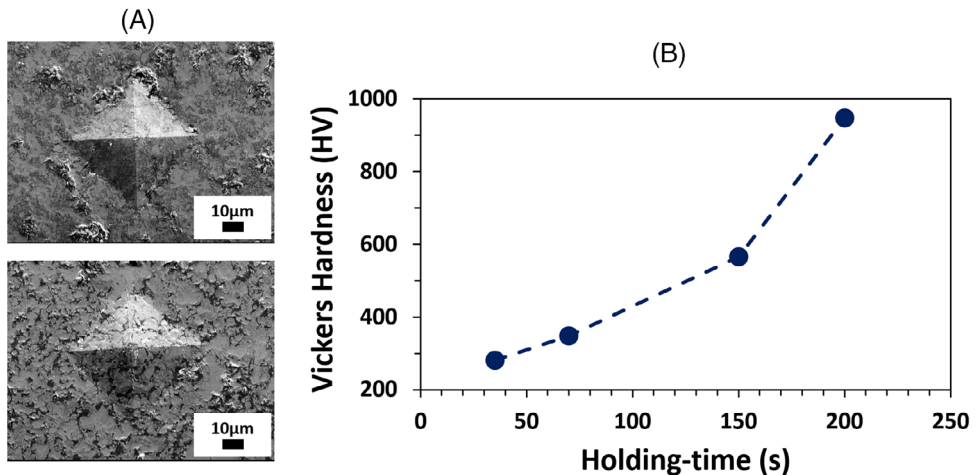


FIGURE 15 (A) Scanning electron microscopy (SEM) micrographs of the Vickers indentations to evaluate the micro-hardness. (B) A plot of micro-hardness values versus post-flash holding time for ZrN samples flash sintered under constant 8 V DC and 15 MPa pressure. Note, only the holding time was varied, whereas other flash sintering (FS) parameters were kept consistent.

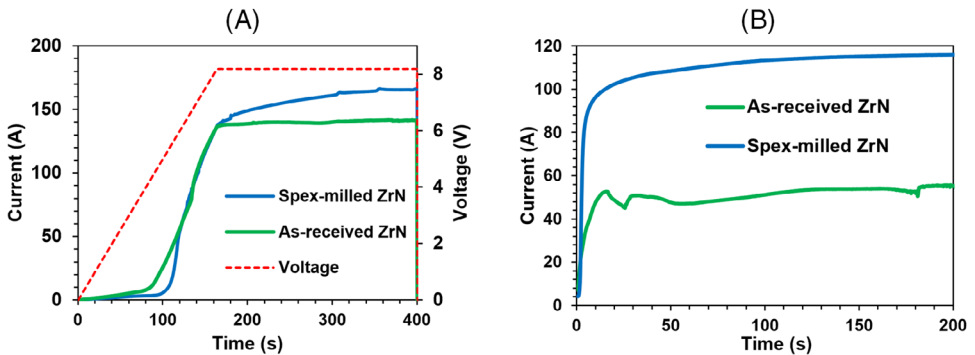


FIGURE 16 Current versus time plots for flash sintering of as-received commercial ZrN powder (green lines) and 5 min Spex-milled (blue line) ZrN powder under 15 MPa of pressure under either (A) linear ramping voltage condition from 0 to 8 V DC at 0.05 V/s or (B) constant 6 V DC condition. Note for both experiments, the samples had been pre-compacted before flash sintering.

reduce the particle size and, possibly, break the (oxide) shells. Due to the high intensity of Spex-milling, it is carried out inside a steel container for only 5 min to avoid contamination. Figure 16 compares the FS behavior for as-received ZrN powder with 5 min Spex-milled ZrN powder, under either (a) 0.05 V/s linear ramping voltage, or (b) constant 6 V DC conditions. In the linear ramping mode (Figure 16A), Spex milling of ZrN powder slightly delayed the onset of the flash event and increased the critical voltage. It also led to an increase in max current. The increase in max current is even more obvious in the constant voltage mode with 6 V DC, as in Figure 16B.

Figure 17A,C shows SEM for as-received ZrN powder and ZrN powder after 5 min Spex-milling, whereas Figure 17B,D shows SEM for fractured surface for flash sintered ZrN samples using the two powders, respectively. Clearly, Spex milling greatly reduced average particle size

from ~5 to 20 μm to submicron and drastically improved densification leading to a near-fully densified sample. (It should be mentioned that planetary ball-milling of ZrN powder in air was also carried out. However, probably due to oxidation during ball-milling after hours long milling, the starting powder became highly resistive, and flash sinter could not be achieved using the current setup.)

The exact reason for the large increase in max current when the ZrN powder is Spex milled is not very clear. One hypothesis is that finer particle size from mechanical milling leads to more surface oxide shell, making the initial resistance higher and delaying the flash. Meanwhile, milling leads to smaller particle size and larger driving force for sintering, which help remove porosity, leading to lower resistance. Detailed studies will be carried out in future to carefully reveal Spex-milling's effect on powder

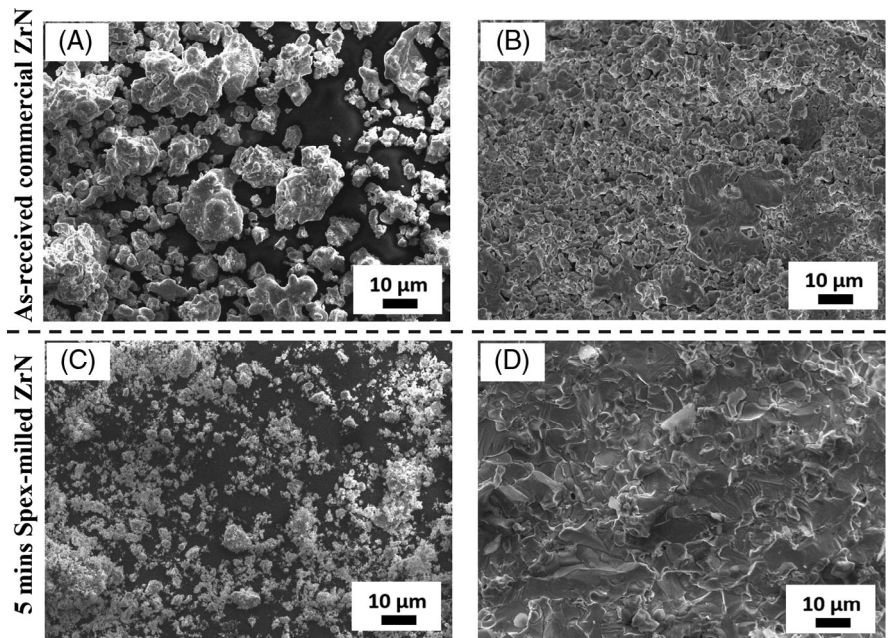


FIGURE 17 Scanning electron microscopy (SEM) micrographs of powders (a and c) and flash sintered samples (b and d) using as-received ZrN powder (141 Å max, a and b), or Spex-milled ZrN (165 Å max, c and d) powders. The flash sintering was carried out at the same condition of 0–8 V DC (ramp up with 0.05 V/s), applied pressure of 15 MPa, and a total time of 400 s. It showed that 5 min Spex-milling greatly reduced the average particle size for the powder and improved densification. (Estimated porosity and grain size are given in Table S1 for information purpose.)

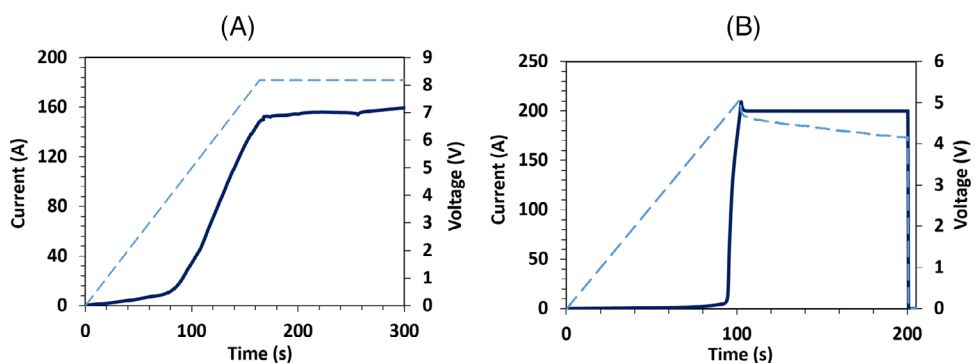


FIGURE 18 Current and voltage trend over time for the flash sintering of ZrN pre-compacted samples under linear ramping voltage at 0.05 V/s and 15 MPa of pressure using (A) graphitic and (B) metallic molybdenum electrodes.

particle size distribution and surface characteristics and their impact on the FS behavior.

3.5 | Effects of electrode materials

The ZrN FS behavior obtained using typical graphitic electrodes is also compared with molybdenum (Mo) electrodes under linear ramping voltage mode, and the results are shown in Figure 18. The flash event—the sudden drastic drop in resistance or increase in current, starts at similar

voltage (~4.5 V DC) when using both electrode materials. However, the transition or the uptake in current is much more gradual when using graphite electrodes, but much more abrupt when using the Mo metal electrode. In addition, when using Mo electrodes, the current reached a higher absolute value and resulted in the transition of the power supply from the voltage-control mode to the current-control mode at 200 A (27 A/mm^2). Afterward, a gradual voltage drop was observed due to the reduction of resistance, probably because of densification leading to lower porosity and reduced apparent resistivity/resistance.

The more drastic increase in current for Mo electrodes suggests that the initial total resistance for Mo before the flash is higher than when using graphite electrodes, but the exact reason is unclear. Given the same powder and applied pressure, one possibility for the difference is that the initial contact resistance between the Mo electrodes and the sample is higher than graphite electrodes. When the threshold electrical field was reached, the electrical contact between Mo electrode and the sample improves drastically and the Mo electrodes yielded higher current due to lower bulk resistivity compared with graphite (17.9×10^4 S/cm for Mo vs. 2 to 3×10^4 S/cm for graphite, both at 20°C). Of course, further experimental investigation is needed to verify this.

Nevertheless, it should be mentioned that despite that Mo metallic electrode gave more abrupt flash behavior, due to the current limit of the power supply, lower voltage (i.e., ~4.5 V) under constant 200 A current meant the total power dissipation for the system was lower—only ~900 W. As a result, the sample temperature was actually lower than when using graphite and the samples did not densify adequately (The sample crumbled easily after FS with Mo electrode. This was in contrast to samples flash sintered using graphite electrode, which were much stronger and mostly survive the extraction process from the sample assembly). For this reason, most studies were carried out using graphite electrodes, instead of Mo. It is also noted that even though Mo is prone to form volatile oxides during heating, the sample assembly containing tightly fit h-BN and graphite parts protects Mo from excessive oxidation.

3.6 | Possibility of repeated flash

It has been reported that oxide ceramics such as YSZ or doped CeO₂ could demonstrate repeated flash, meaning that after the first flash event, the flash-sintered sample could display flash-like behavior again when it is subject to the same temperature and electrical voltage condition.¹² The repeated flash is due to the large (Arrhenius-type) increase of intrinsic conductivity with increasing temperature for oxide materials (see Figure 2A). In this study, we investigated if a second (or repeated) flash would occur for highly conductive ZrN HTC material. For this, a typical ZrN FS experiment was first carried out and the system was then cooled down naturally to room temperature. Keeping the sample in place, the same linear voltage ramp from 0 to 8 V DC was applied to the flash-sintered ZrN sample again and the change in current was recorded.

Figure 19A shows the change of total resistance versus time for the ZrN sample for both the first flash event and the second cycle. As before, for the first flash event, the total resistance dropped dramatically from ~0.6 Ω (at 1.2 s)

to 0.06 Ω (at 94.7 s), representing the flash event. After the sample cooled down, the same voltage was applied again, but the flash-sintered ZrN did not seem to experience another flash: The resistance started very low (~0.1 Ω) and there was only a very minor decrease in total resistance, which was probably more related to better contacts between different parts including the sample and the multiple graphite electrodes, instead of anything happening within the sample. In fact, subsequent trials on graphite electrodes alone without ZrN powder compact display the same ~50% decrease in resistance, as in the second cycle.

3.7 | Considerations on potential ZrN flash sintering mechanism

The observed FS behaviors for ZrN have some implications for the ZrN FS mechanism. In particular, though most researchers agree that the flash event involves runaway Joule heating, some have proposed point defect accumulation as the trigger before the flash. The comparison of ZrN flash behavior between different electrodes of graphite versus Mo suggests that it is unlikely that defects accumulation plays a significant role in ZrN FS since during the incubation stage: The amount of total electrical energy dissipation was only half when using the Mo electrode (estimated to be ~890 J when using Mo electrode vs. ~1730 J when using graphite electrode, assuming, as a first approximation, linear current increase before flash), yet the FS behavior is more significant with Mo electrode. In addition, due to the low voltage/electrical field involved, ZrN flash was unlikely to be triggered by excess defects in the ZrN lattice generated by electrical field.

On the other hand, the absence of repeated flash is consistent with the displayed intrinsic or bulk (for 100% dense sample) conductivity for ZrN: The *bulk* conductivity actually decreases slightly with increasing temperature (see Figure 2A), which would not enable the self-accelerating heating effect under constant voltage condition. It also indicates that observed FS for ZrN in this study as well as our earlier report is not due to the change in ZrN bulk conductivity with temperature. Instead, it is hypothesized the improved ZrN particle contacts and/or breakdown of less conductive surface layer (e.g., surface oxide shell) over the ZrN particle surface upon heating and/or mechanical compaction lead to the large drop in resistance and the accompanied flash for such highly conductive HTC of ZrN. Apart from bulk conductivity, one of the major differences between oxides like YSZ and highly conductive HTC like ZrN is that the latter is easily subject to oxidation in the open air. No matter the synthesizing process, it is inevitable to have oxides, often as surface layers, on ZrN particles.^{40,41} (In fact, the 6 wt.% of ZrO₂ impurity in the starting ZrN

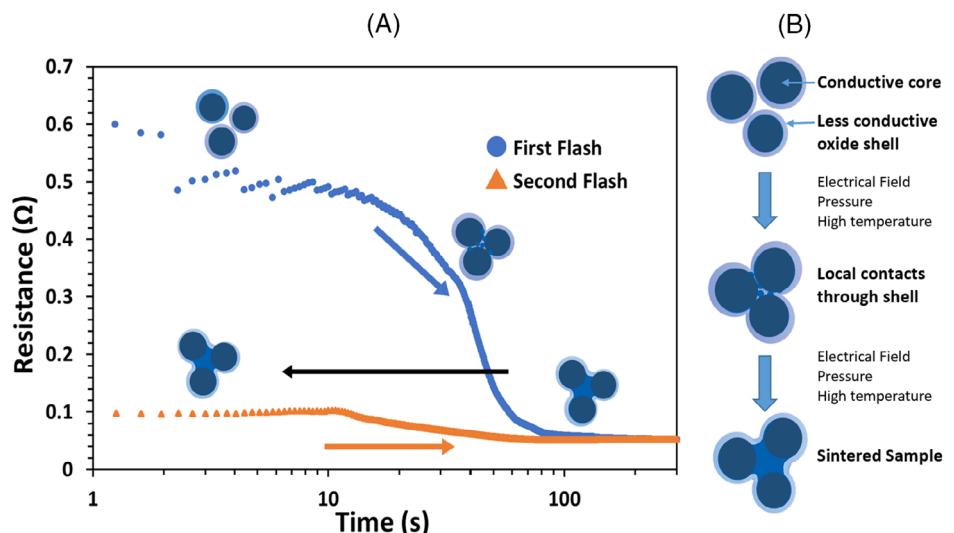


FIGURE 19 (A) Total resistance versus time for the first and second attempts of flash on the same ZrN sample. The voltage applied was linearly ramped up from 0 to 8 V DC at 0.1 V/s and the pressure was 15 MPa pressure for both attempts. (B) Schematic showing hypothesized change in the sample's microstructure during ZrN powder flash sintering.

powder, as determined by Rietveld analysis, would correspond to an estimated ZrO_2 surface layer of ~ 24 nm thick, if assuming 1 μm diameter primary particles.) Compared with metallic conducting ZrN, the oxides (e.g., ZrO_2) are almost insulating at room temperature. Therefore, it is possible when the particles are only lightly touching each other, the sample would have remarkably high apparent resistivity due to both porosity and surface oxides.

It is hypothesized that upon Joule heating, mechanical compaction, or both, breakdowns of the (oxide or other) shell surrounding the ZrN might occur. Or the oxide shells might go through localized Joule heating. At a certain voltage (or electric field strength) and/or temperature at the boundaries, an electrical breakthrough occurs, and resistance drops suddenly, and the flash happens subsequently. Figure 19B is a schematic illustrating the hypothesized changes that include both enhanced contacts or better packing and breakage of oxide shell for ZrN material during FS.

It must be mentioned that such a hypothesis is consistent with some very recent studies on FS for tungsten carbide as well as metallic tungsten that suggest the critical role of less conductive surface layer (amorphous carbon or oxide) over conductive powder surface in enabling the flash event for these materials.^{19,21,42,43} Further verification using both extensive materials characterization and computation modeling based on the finite element method will be carried out in the future to verify such a hypothesis and, possibly distinguish the contributions from particle packing/densification and fracture or breakdown of low conductivity (oxide or other) shells.

Finally, when comparing flash for highly conductive high temperature ceramics like ZrN and flash for con-

ventional oxides such as YSZ, we believe the overall mechanism is the same: a drastic reduction in apparent total resistance with temperature. However, for conventional oxides like YSZ, the drop in apparent resistance with temperature may come from two parts: bulk conductivity and reduced porosity/better contacts. In fact, repeated flash will occur for post FS oxide samples as well as single crystal (100% dense) oxides.⁴³ For highly conductive HTC like ZrN, the drop in apparent resistance cannot come from the drop in bulk conductivity with temperature for such materials. Instead, it comes only from the improved contacts and, possibly, cracking and contact through of the less conductive surface layer (e.g., oxides). Of course, this also needs to be verified in future through detailed experiments including extensive materials characterization as well as modeling.

4 | CONCLUSIONS

In the presented study a series of experiments were conducted to investigate the FS behavior for ZrN—a highly conductive HTC material. The effects of different processing parameters from the voltage (or electrical field strength) and voltage ramp rate to post-flash holding time and mechanical pressure were qualitatively investigated. The results show that there was no flash when voltage was below a certain value (~ 5 V), whereas higher voltage (e.g., 8 V) led to a drastic increase in maximum current, representing the nonlinear effect of typical FS. The ramp rate did not change the critical voltage, indicating the electrical field instead of accumulated heat plays a critical role in triggering the flash. Longer post-flash holding

time helped densification (for the limited power supply used), but its effect was not as significant as the electrical field strength and the maximum current (density) reached. Flash occurred at pressure as low as 3 MPa with 6.4 V DC, indicating that, similar to oxides like YSZ, pressure does not seem necessary for the flash event to occur for ZrN. However, higher pressure does shorten the incubation time and increased the maximum current density, leading to much-improved densification (up to ~25 MPa). Reducing particle size through short-time (e.g., 5 min) Spex milling increased max current and substantially improved densification. Changing electrode materials influenced the observed flash behavior with graphite electrodes giving gradual flash but better densification, whereas Mo enables more abrupt flash, but less densification. Repeated flash for ZrN was not observed, which is contrary to oxides such as YSZ. Finally, there was significant variation in the FS experiments, and both the setup and the process need to be improved for better consistency.

The observed FS behaviors for ZrN suggest that it shares similarities as well as differences from conventional oxides such as YSZ. One possible hypothesis for the occurrence of the flash event for highly conductive HTC of ZrN is it might be due to the improved contacts and breakage/breakdown of less conductive surface shells (possibly oxides) over ZrN surfaces, which leads to significantly reduced resistivity.

It is noted that there are still many important unknowns with respect to FS of ZrN, especially in terms of sintering kinetics, that is, how samples relative density or porosity change with FS parameters (e.g., applied voltage and resulting current density, post flash holding time) in a quantitative way. Studies are also needed to optimize the various steps from commercial powder pre-processing (e.g., Spex-milling) to actual FS. In addition, both theoretical modeling and detailed materials characterization, especially quantitative analysis of particle size distribution, particle morphology and surface *atomic-scale structure and stoichiometry*, precise measurements of flash sintered samples' relative density/porosity, pore size and shape, grain size and shape, are all needed. Continued study should aim at testing the above hypothesis concerning the origin of FS for highly conductive HTC materials such as ZrN, understanding the complex composition-processing-structure relationship, and distinguishing the contributions by improved particle packing from the breakage/breakdown of the less conductive (oxide) surface layers.

ACKNOWLEDGMENTS

This work was supported by the U.S. Department of Energy (DOE), Office of Science, Basic Energy Science, Grant No. DE-SC0022152. Author KS thanks Florida International University (FIU) Graduate School for the Presidential Fellowship (PF) award.

ORCID

Suprabha Das  <https://orcid.org/0000-0002-4087-2474>

REFERENCES

- Harrison RW, Lee WE. Processing and properties of ZrC, ZrN and ZrCN ceramics: a review. *Adv Appl Ceram.* 2016;115:294–307. <https://doi.org/10.1179/1743676115Y.0000000061>
- Pejaković V, Totolin V, Göcerler H, Brenner J, Rodríguez Ripoll M. Friction and wear behaviour of selected titanium and zirconium based nitride coatings in Na₂SO₄ aqueous solution under low contact pressure. *Tribol Int.* 2015;91:267–73.
- Adachi J, Kurosaki K, Uno M, Yamanaka S. Thermal and electrical properties of zirconium nitride. *J Alloys Compd.* 2005;399:242–44.
- Tang Y, Zhang G-J, Xue J-X, Wang X-G, Xu C-M, Huang X. Densification and mechanical properties of hot-pressed ZrN ceramics doped with Zr or Ti. *J Eur Ceram Soc.* 2013;33:1363–71.
- Bram M, Laptev AM, Mishra TP, Nur K, Kindelmann M, Martin I, et al. Application of electric current-assisted sintering techniques for the processing of advanced materials. *Adv Eng Mater.* 2020;22:2000051.
- Dancer CEJ. Flash sintering of ceramic materials. *Mater Res Express.* 2016;3:102001.
- Biesuz M, Sglavo VM. Flash sintering of ceramics. *J Eur Ceram Soc.* 2019;39:115–43.
- Cologna M, Prette ALG, Raj R. Flash-sintering of cubic yttria-stabilized zirconia at 750°C for possible use in SOFC manufacturing. *J Am Ceram Soc.* 2011;94:316–19.
- Cologna M, Rashkova B, Raj R. Flash sintering of nanograin zirconia in <5 s at 850°C. *J Am Ceram Soc.* 2010;93:3556–59.
- Yu M, Grasso S, McKinnon R, Saunders T, Reece MJ. Review of flash sintering: materials, mechanisms and modelling. *2016;116:24–60.* <https://doi.org/10.1080/17436753.2016.1251051>
- Raj R. Analysis of the power density at the onset of flash sintering. *J Am Ceram Soc.* 2016;99:3226–32.
- Caliman LB, Bichaud E, Soudant P, Gouvea D, Steil MC. A simple flash sintering setup under applied mechanical stress and controlled atmosphere. *MethodsX.* 2015;2:392–98.
- Grasso S, Saunders T, Porwal H, Milsom B, Tudball A, Reece M. Flash spark plasma sintering (FSPS) of α and β SiC. *J Am Ceram Soc.* 2016;99:1534–43.
- Foroughi P, Durygin A, Sun S, Cheng Z. Flash sintering of tantalum-hafnium diboride solid solution powder. *J Mater Res.* 2022;37:2150–56. <https://doi.org/10.1557/S43578-022-00492-7>
- Francis JSC, Raj R. Flash-sinterforging of nanograin zirconia: field assisted sintering and superplasticity. *J Am Ceram Soc.* 2012;95:138–46.
- Das S, Dubois D, Sozal MdSI, Emirov Y, Jafarizadeh B, Wang C, et al. Synthesis and flash sintering of zirconium nitride powder. *J Am Ceram Soc.* 2022;105:3925–36.
- Mondal S, Durygin A, Drozd V, Belisario J, Cheng Z. Multi-component bulk metal nitride (Nb_{1/3}Ta_{1/3}Ti_{1/3})N_{1-δ} synthesis via reaction flash sintering and characterizations. *J Am Ceram Soc.* 2020;103:4876–93.
- Belisario J, Mondal S, Khakpour I, Franco Hernandez A, Durygin A, Cheng Z. Synthesis and flash sintering of (Hf_{1-x}Zr_x)B₂ solid solution powders. *J Eur Ceram Soc.* 2021;41:2215–25.

19. Mazo I, Molinari A, Sglavo VM. Electrical resistance flash sintering of tungsten carbide. *Mater Des*. 2022;213:110330.
20. Mazo I, Molinari A, Sglavo VM. Effect of pressure on the electrical resistance flash sintering of tungsten carbide. *J Eur Ceram Soc*. 2022;42:2028–38.
21. Deng H, Biesuz M, Vilémová M, Kermani M, Veverka J, Tyrpekl V, et al. Ultrahigh temperature flash sintering of binder-less tungsten carbide within 6 s. *Materials (Basel)*. 2021;14:7655.
22. Das S, Durygin A, Drozd V, Sozal MdSI, Cheng Z. Reactive flash sintering of TiZrN and TiAlN ternary metal nitrides. *J Eur Ceram Soc*. 2024;44:2037–51.
23. Raj R, Wolf DE, Yamada CN, Jha R, Lebrun J-M. On the confluence of ultrafast high-temperature sintering and flash sintering phenomena. *J Am Ceram Soc*. 2023;106:3983–98.
24. Mazo I, Molinari A, Sglavo VM. Electrical resistance flash sintering of tungsten carbide. *Mater Des*. 2021;213:110330.
25. Ahamer C, Opitz AK, Rupp GM, Fleig J. Revisiting the temperature dependent ionic conductivity of yttria stabilized zirconia (YSZ). *J Electrochem Soc*. 2017;164:F790–F803.
26. Todd RI, Zapata-Solvias E, Bonilla RS, Sneddon T, Wilshaw PR. Electrical characteristics of flash sintering: thermal runaway of Joule heating. *J Eur Ceram Soc*. 2015;35:1865–77.
27. Serrazina R, Vilarinho PM, Senos AMOR, Pereira L, Reaney IM, Dean JS. Modelling the particle contact influence on the Joule heating and temperature distribution during FLASH sintering. *J Eur Ceram Soc*. 2020;40:1205–11.
28. Narayan J. A new mechanism for field-assisted processing and flash sintering of materials. *Scr Mater*. 2013;69:107–11.
29. Charalambous H, Jha SK, Wang H, Phuah XL, Wang H, Tsakalakos T. Inhomogeneous reduction and its relation to grain growth of titania during flash sintering. *Scr Mater*. 2018;155:37–40.
30. Ren K, Huang S, Cao Y, Shao G, Wang Y. The densification behavior of flash sintered BaTiO₃. *Scr Mater*. 2020;186:362–65.
31. Zhou H, Li X, Zhu Y, Liu J, Wu A, Ma G, et al. Review of flash sintering with strong electric field. *High Volt*. 2022;7:1–11.
32. Biesuz M, Pinter L, Saunders T, Reece M, Binner J, Sglavo V, et al. Investigation of electrochemical, optical and thermal effects during flash sintering of 8YSZ. *Materials (Basel)*. 2018;11:1214.
33. Biesuz M, Luchi P, Quaranta A, Sglavo VM. Theoretical and phenomenological analogies between flash sintering and dielectric breakdown in α -alumina. *J Appl Phys*. 2016;120:145107.
34. Liu J, Rongxia H, Zhang R, Liu G, Wang X, Jia Z, et al. Mechanism of flash sintering with high electric field: In the view of electric discharge and breakdown. *Scr Mater*. 2020;187:93–96.
35. Rahman M, Wang CC, Chen W, Akbar SA, Mroz C. Electrical resistivity of titanium diboride and zirconium diboride. *J Am Ceram Soc*. 1995;78:1380–82.
36. Taylor RE. Thermal conductivity of zirconium carbide at high temperatures. *J Am Ceram Soc*. 1962;45:353–54.
37. Adachi J, Kurosaki K, Uno M, Yamanaka S. Effect of porosity on thermal and electrical properties of polycrystalline bulk ZrN prepared by spark plasma sintering. *J Alloys Compd*. 2007;432:7–10.
38. Luo J. The scientific questions and technological opportunities of flash sintering: from a case study of ZnO to other ceramics. *Scr Mater*. 2018;146:260–66.
39. Gorynski C, Anselmi-Tamburini U, Winterer M. Controlling current flow in sintering: a facile method coupling flash with spark plasma sintering. *Rev Sci Instrum*. 2020;91:015112.
40. Saha NC, Tompkins HG. Titanium nitride oxidation chemistry: an x-ray photoelectron spectroscopy study. *J Appl Phys*. 1998;72:3072.
41. Glaser A, Surnev S, Netzer FP, Fateh N, Fontalvo GA, Mitterer C. Oxidation of vanadium nitride and titanium nitride coatings. *Surf Sci*. 2007;601:1153–59.
42. Alan Weimer RR. Conventional and flash sintering of tungsten and tungsten alloys prepared by robocasting of ald-doped precursors. NASA. (2021). <https://www.nasa.gov/directories/stmd/space-tech-research-grants/conventional-and-flash-sintering-of-tungsten-and-tungsten-alloys-prepared-by-robocasting-of-ald-doped-precursors/>
43. Mazo I, Vanzetti LE, Molina-Aldareguia JM, Molinari A, Sglavo VM. Role of surface carbon nanolayer on the activation of flash sintering in tungsten carbide. *Int J Refract Met Hard Mater*. 2023;111:106090.

SUPPORTING INFORMATION

Additional supporting information can be found online in the Supporting Information section at the end of this article.

How to cite this article: Eskandariyun A, Das S, Dubois D, Saeedian K, Durygin A, Drozd V, et al. Effects of processing conditions on flash sintering of commercial ZrN. *J Am Ceram Soc*. 2024;107:3735–50. <https://doi.org/10.1111/jace.19719>